

**The effect of anionic clay particles on the structure and thermomechanical behavior of sodium partially-neutralized EMAA ionomer**

Journal:	<i>Journal of Applied Polymer Science</i>
Manuscript ID:	APP-2009-09-2788
Wiley - Manuscript type:	Research Article
Keywords:	ionomers, thermal properties, clay



Review

**The effect of anionic clay particles on the structure and thermomechanical behavior of sodium partially-neutralized EMAA ionomer**

**M. Ardanuy\***

[Monica.ardanuy@upc.edu](mailto:Monica.ardanuy@upc.edu)

Escola Tècnica Superior d'Enginyeries Industrial i Aeronàutica de Terrassa

Universitat Politècnica de Catalunya.

C/ Colom, 11. E-08222 Terrassa (Spain)

**J.I. Velasco**

[jose.ignacio.velasco@upc.edu](mailto:jose.ignacio.velasco@upc.edu)

Centre Català del Plàstic. Universitat Politècnica de Catalunya

C/ Colom 11, E-08222 Terrassa (Spain)

**M.A. Rodriguez-Perez**

[marrod@fmc.uva.es](mailto:marrod@fmc.uva.es)

Departamento de Física de la Materia Condensada, Cristalografía y Mineralogía. Facultad de Ciencias.

Universidad de Valladolid.

Prado de la Magdalena s/n, 47011 Valladolid (Spain)

**J.A. de Saja**

[sajasaez@fmc.uva.es](mailto:sajasaez@fmc.uva.es)

Departamento de Física de la Materia Condensada, Cristalografía y Mineralogía. Facultad de Ciencias.

Universidad de Valladolid.

Prado de la Magdalena s/n, 47011 Valladolid (Spain)

\*Corresponding author: [monica.ardanuy@upc.edu](mailto:monica.ardanuy@upc.edu)

Tel. (+34) 93 739 81 58

Fax (+34) 93 739 81 01

## **The effect of anionic clay particles on the structure and thermomechanical behavior of sodium partially-neutralized EMAA ionomer**

### **Abstract**

Nanocomposites based on a sodium partially-neutralized ionomer of poly (ethylene-co-methacrylic acid) (EMAA) and MgAl layered double hydroxide (LDH) particles with and without organic modification were prepared from a melt mixing process. The structure was characterized using X-ray diffraction analysis (XRD) and transmission electron microscopy (TEM). Although TEM micrographies revealed the presence of agglomerates of LDH sheets, the achievement of an exfoliated structure was observed when dodecyl sulphate-modified LDH particles were used. The effects of the LDH particles on the thermomechanical properties of EMAA were analyzed using differential scanning calorimetry (DSC) and dynamic mechanical thermal analysis (DMTA). The thermal transition of the ionic aggregates and dynamic mechanical response of EMAA were found strongly modified by these particles, resulting in an increase on the storage modulus and a decrease on the loss factor values. Moreover, the alpha relaxation of the composites was visibly shifted to higher temperatures.

Keywords: layered double hydroxides; thermomechanical properties; ionomer; poly (ethylene-co-methacrylic acid).

## INTRODUCTION

Ionomers are polymers with a small mole fraction of ionic groups covalently bonded to the polymer backbone. Ethylene ionomers consisting of polyethylene and methacrylic acid groups partially neutralized with sodium or zinc ions (EMAA) are the most commonly used in industrial applications. These applications include packaging films and sealants, glass coatings and abrasion resistant surfaces and buoys. Moreover, ionomer-based materials carry great potential for use in a wide variety of unique applications because of their “self-healing” behavior<sup>1</sup>.

The use of cationic clays as precursors of polymer nanocomposites has been recently extended to the family of layered double hydroxides (LDHs)<sup>2-6</sup>. These particles, also known as “anionic clays”, are lamellar compounds containing exchangeable anions. Their structure consists of brucite-like  $M(OH)_2$  sheets, in which the partial substitution of trivalent for divalent cations results in a positive charge compensated by anions within the interlayer space. LDHs are represented by the general formula:  $[M^{2+}_{1-x} M^{3+}_x (OH)_2][A^{n-}_{x/n} \cdot mH_2O]$ , where  $M^{2+}$  and  $M^{3+}$  are di- and trivalent metal ions respectively, which occupy octahedral positions in the hydroxide layers, and  $A^{n-}$  is an interlayer anion<sup>7</sup>. The nature of the metal ions can be chosen from a wide number of options (for instance,  $Mg^{2+}$ ,  $Ni^{2+}$ ,  $Zn^{2+}$ ;  $Al^{3+}$ ,  $Fe^{3+}$  and  $Mn^{3+}$  among others), and the interlayer anion can be also chosen from either inorganic or organic species. Anionic clays might offer advantages over cationic clays, such as montmorillonite because of its versatility in chemical composition and modifiable charge density. Moreover, LDH sheets consist of only one polyhedra-made layer, often corrugated, and are, therefore, more flexible than other silicate-layered particles such as montmorillonite.

The thermomechanical properties of polymer clay nanocomposites are determined by the complex relationship between the nature and size of the particles, hybrid interface and nature of the interactions between the organic and inorganic components. That is why the increase in the specific contact surface of the layered particles with the polymer matrix through exfoliation and promotion of higher interactions between the clay platelets and polymeric matrix are of such importance.

On one hand, the increase in the specific contact surface in the melt mixing preparation procedure includes the clay organophilization, consisting of swelling via the ion-exchange process with organic ions, followed by dispersion into a polymer matrix by applying high local shear stresses in a melt mixer dispositive. These organophilized particles display an expanded crystalline structure because of the higher free volume of the interlamellar organic ion.

On the other hand, it is usually necessary to use polar polymers or polar compatibilizer agents to promote strong interactions between the polymer melt and clay particles. Different studies have proven the effectiveness of EMAA ionomers as compatibilizers in polyethylene/montmorillonite nanocomposites<sup>12-14</sup>. This effectiveness has been attributed to the interactions of the ionic and acid groups in these ionomers with the aluminosilicate surface of the clay. In similar way, EMAA/LDH nanocomposites could be interesting systems because of the expected favorable interactions between the LDH sheets (positively charged) and ionic groups on the ionomer (negatively charged).

Dynamic mechanical thermal analysis (DMTA) has been widely employed to study the structure and viscoelastic behavior of polymers and, more specifically, polymer composite materials. The DMTA technique can also be used to follow main

chain and side-group motions and is particularly useful for studying thermal transitions of polymers. For a better understanding of the dynamic mechanical properties of the nanocomposites it would be helpful to study the effects of LDH particles on the thermal and mechanical properties of EMAA ionomers.

In this paper, EMAA nanocomposites containing pure and organically-modified LDH particles have been prepared via the melt mixing process and the effects induced by these particles on the structure and thermomechanical properties analyzed.

## EXPERIMENTAL

### Materials

A sodium EMAA ionomer, Surlyn 8920, manufactured by Dupont, with a 5.4 mol% of acid groups partially neutralized (60%) was used as a polymer matrix.

Synthetic magnesium aluminium LDH (hydrotalcite) supplied by Ciba (Hycite 713) with a formula  $[\text{Mg}_{0.7}\text{Al}_{0.3}(\text{OH})_2](\text{CO}_3)_{0.15}\cdot n\text{H}_2\text{O}$  was used as a LDH precursor. Sodium dodecyl sulphate was purchased from the Aldrich Chemical Company.

Structure-expanded organophilized LDH particles (O-LDH) containing dodecyl sulphate anions into the interlamellar space were prepared according to a previously published procedure<sup>10</sup>.

### Nanocomposite preparation

Nanocomposites containing pure (LDH) and organically-modified LDH particles (O-LDH) (90/10 by weight) were prepared by the melt mixing process using a co-rotating twin-screw extruder (Collin ZK-35) of diameter 25 mm and a length to

diameter ratio of 36. To apply a high shearing level to promote LDH exfoliation, different kneading blocks were inserted into the screw configuration. The screw speed was fixed at 60 rpm and the temperature profile in the barrel was so that the melt temperature remained under 160°C at the extruder die, as measured by the mass transducer. A circular cross-section die of 3 mm diameter was employed. The extrudate was cooled in a water bath and pelletized. Circular plates of the composite pellets of diameter 75 mm and thickness 3 mm were compression-molded using a hot-plate press at 135°C for 3 min. The samples were cooled under pressure for 10 min. In this molding cycle, the maximum applied pressure was 95 bar.

### Testing and measurements

With the aim of evaluating the interlamellar space in the O-LDH crystal to gain information about the exfoliation of nanoplatelets, X-ray diffraction analysis (XRD) was performed on both the LDH powders and the prismatic samples ( $25 \times 5 \times 3 \text{ mm}^3$ ) machined from the molded circular plates. Data were collected on the  $2\theta$  range from 2–60°, 0.02°/min scan increments (operating at 40 KV and 30 mA). A Siemens D-500 diffractometer was employed with  $\text{CuK}\alpha$  radiation ( $\lambda = 0.154 \text{ nm}$ ). The interlamellar spacing in the O-LDH was calculated from the (003) interplanar distance, according to the Bragg equation. The diffraction planes of LDH and O-LDH were indexed-based on a hexagonal unit cell.

Information about the morphology and distribution of the O-LDH particles was obtained from observations using a JEOL 1200-EXII transmission electron microscope. Ultramicrotomed samples with a typical thickness of 100–200 nm were employed.

Analysis of the thermal transitions of EMAA ionomers was carried out by differential scanning calorimetry (DSC). Measurements were performed using a Perkin-Elmer Pyris 7 calorimeter on samples aged for four months at room temperature. Calibration of the instrument was done using standard samples of indium and lead. Experiments consisted of heating from 25°C to 160°C and then cooling to 20°C, both processes at a rate of 10°C/min. All runs were carried out in a stream of dried nitrogen. Samples of 10 mg were used in each case.

DMTA tests were carried out using two kinds of testing configurations: shear and three-point bending modes.

The three-point bending mode was carried out using a Perkin-Elmer DMTA 7, which was calibrated according to the standard procedure. The samples employed were the same as those used in XRD measurements. A static stress of 0.6 MPa and a dynamic stress of  $\pm 0.5$  MPa were applied with a frequency of 1 Hz. Firstly, dynamic loading was isothermally applied at  $22 \pm 1^\circ\text{C}$  to gain quantitative results of the storage modulus ( $E'$ ) and loss tangent ( $\tan \delta$ ). The values were taken 5 min after applying the stresses and four measurements were registered for each material. Secondly, the study of the secondary relaxations was carried out through tests performed in temperature range of –150 to 60 °C, at a heating rate of 5°C/min.

The shear mode was performed using a DMA 861 Mettler. Samples employed were of rectangular geometry ( $5 \times 3 \times 3 \text{ mm}^3$ ) machined from the discs. Firstly, a dynamic force of 16 N at 1 Hz was isothermally applied at  $22 \pm 1^\circ\text{C}$  to gain quantitative results of the storage modulus ( $G'$ ) and loss tangent ( $\tan \delta$ ). The values were taken 10 min after applying the stresses, i.e., once the initial fluctuations of the values had disappeared. To ensure reproducibility, three measurements were registered for each

material. Secondly, non-isothermal measures were performed on the temperature range  $-160^{\circ}\text{C}$  to  $100^{\circ}\text{C}$  (heating rate of  $5^{\circ}\text{C}/\text{min}$ ) to study the secondary relaxations.

To obtain information about the degree of interaction between the nanoparticles and ionomer on melt state, melt flow index (MFI) measures were performed on a melt flow indexer, according to ASTM D-1238 ( $190^{\circ}\text{C}$  and 2.16 Kg).

## RESULTS AND DISCUSSION

### Structure and morphology

The comparison of XRD spectra of pure and organically-modified LDH particles showed an expanded crystalline structure in the O-LDH sample along the [001] crystalline direction (or  $c$ -axis) (Figure 1). The insertion of dodecyl sulphate ion (DS) into the LDH gallery resulted in a shift of the (003) diffraction peak from  $2\theta = 11.48^{\circ}$  (pure LDH) to  $2\theta = 3.33^{\circ}$  (O-LDH sample). This shift was related to an increase in the  $d$  spacing ( $d_{003}$ ) of the LDH crystal from 0.77 to 2.65 nm. The  $d_{003}$  value includes a contribution of the metal hydroxide sheet thickness (typically  $4.8 \text{ \AA}^{11}$ ) and gallery height, which contains the anions and other possible intercalated molecules. As shown, the incorporation of the dodecyl sulphate anions resulted in a significant increase in gallery height. As the LDH thickness was unaffected by DS incorporation, the expansion of the LDH structure along the  $c$ -axis caused the unit cell volume to expand. Because of this structure expansion, and despite the higher mass of the DS ion than that of the carbonate one, the density of LDH particles was found to pass from  $2.07 \text{ g/cm}^3$  for the precursor to  $1.54 \text{ g/cm}^3$  for the organophilized particles. It is expected that this larger space between the LDH layers will promote the intercalation of the polymer, leading to easy exfoliation of the LDH sheets in the ionomer matrix.

Figure 2 shows the XRD spectra of EMAA ionomer and nanocomposites. As shown, pure EMAA presents two broad signals at  $4.2^\circ$  and  $20.7^\circ$ . The first is related to the formation of ionic aggregates (known as *ionic signal*) and the second results from the overlapping of the diffraction signals assigned to the polyethylene phase. The XRD pattern of EMAA-LDH nanocomposites shows the superposition of both LDH and EMAA diffraction signals, indicating that pure LDH particles maintain their original structure into the EMAA matrix. By contrast, on the pattern of EMAA-O-LDH the diffraction signals of the O-LDH particles disappeared. Therefore, the results show that the nanoparticles were exfoliated into the ionomer matrix. Moreover, the widening of the ionic signal of EMAA in this sample suggests a disarrangement of the ionic aggregates. This disarrangement could be caused by strong interactions between the ionic groups in the ionomer and the O-LDH sheets, which would act as counterions (Figure 3).

By contrast, an increase of the full-width at half-maximum values of the diffraction signal assigned to the polyethylene phase was observed in both nanocomposites with respect to the pure EMAA ( $4.9^\circ$  for both EMAA-LDH and EMAA-O-LDH and  $4.6^\circ$  for EMAA). This widening is because of the higher inhomogeneity of the polyethylene phase in the nanocomposites.

A TEM micrograph (Figure 4 a) of the EMAA-O-LDH sample confirmed the exfoliation of the O-LDH platelets on a EMAA matrix. Moreover, evident agglomeration of the exfoliated LDH platelets occurred (Figure 4 b). The tendency of the nanoplatelets to agglomerate themselves is the basis for the strong ionic interaction forces between the ionomer methacrylic groups and positively charged LDH platelets (Figure 4 b).

### **Melt flow behavior**

The MFI of EMAA was strongly modified by the effect of the LDH particles passing from 0.94 g/10 min for pure EMAA to 0.08 and 0.07 g/10 min for EMAA–LDH and EMAA–O–LDH nanocomposites respectively. This constraint of the EMAA melt flow at low shear rates observed in both nanocomposites can be explained by the existence of strong ionic interaction forces between the positively charged LDH platelets and MAA groups of the ionomer in the melt state. In this sense, Vanhoorne et al.<sup>12</sup> justify the melt flow behavior of ionomers based on a mechanism known as “ion-hopping”. The diffusion (“hopping”) of ionic groups among the ionic aggregates permits the relaxation of stresses within the segment of the polymer chain attached to the ionic group. In ionomers, the ionic associations, which act as a physical crosslink, reduce the diffusion coefficient of the molecules, resulting in increased viscosity. In the nanocomposites under study, the aforementioned significant increase in the viscosity can be attributed to the substitution of sodium as counterions by the positively charged LDH platelet ones, which would hinder the flow of the MAA groups between aggregates.

### **Thermal transitions**

The two typical thermal transitions of EMAA ionomers could be observed in DSC thermograms (Figure 5). The first one, around 50°C, is assigned to the *order–disorder* transition of the ionic clusters. The second one, around 90°C, is related to the melting of polyethylene crystal<sup>13,14</sup>. As shown, the order–disorder transition shifted from 51.3°C for pure EMAA to 54.7°C and 56.0°C for EMAA–LDH and EMAA–O–

LDH nanocomposites respectively. As mentioned, this transition is ascribed to the disarrangement of the ionic aggregates. So, the increase observed on the temperature of this thermal transition could be explained by the formation of more stable ionic aggregates when both pure and organically-modified LDH particles are present in the material. This effect was more noticeable with O-LDH particles.

Concerning to the second transition, a slight shift to lower temperatures was observed in the nanocomposites. This shift is related to the formation of a less robust crystalline phase in these materials, in agreement with the aforementioned widening of the polyethylene phase diffraction signal observed in XRD patterns.

To determine the influence of aging time on the order–disorder behavior of pure and EMAA nanocomposites, complementary DSC experiments were carried out on the materials after different annealing periods (5 min, 10 min, 40 min, 4 h, 14 h and 48 d). Figure 6 shows the general behavior observed in thermograms registered. As expected<sup>13,14</sup> because of an ordering process, with the increasing of the aging time the enthalpy of the order–disorder transition peak increases and the maximum shifts to the higher temperatures (Figure 6). Nevertheless, LDH particles induced faster ordering behavior of ionic clusters, mainly when the organophilized ones were used (Table 1).

### **Dynamic mechanical thermal behavior**

The values of storage modulus ( $E'$  and  $G'$ ) and loss factor values ( $\tan \delta$ ) obtained from isothermal tests at 20°C are presented in Table 2. The glassy storage modulus of the nanocomposites was significantly higher than the one for neat EMAA, mainly when the O-LDH particles were used. This behavior can be attributed to the movement limitation of the EMAA polymer near the LDH particles because of the

strong interactions between the LDH platelets and MAA ionic groups, leading to a good transfer stress from the matrix to the particles.

By contrast, the loss factor values decreased in the nanocomposites. This decrease, mainly observed on the three-point bending mode, could be related to the higher restricted mobility of the EMAA matrix because of the effects induced by the LDH particles. This behavior is in agreement with the aforementioned results. The formation of stronger ionic aggregates from the effects of LDH particles leads to an amorphous polyethylene phase with more restricted mobility.

Figure 7 illustrates the variation of the storage modulus and the loss factor value with the temperature measured with the three-point bending mode test. Two main relaxations could be seen on the loss factor value curves: the first ( $\gamma$  relaxation) around  $-120^{\circ}\text{C}$  and the second ( $\alpha$  relaxation) around  $-10^{\circ}\text{C}$ .  $\gamma$  relaxation is related to the local molecular movement of the chain segments on the amorphous phase and is ascribed to the glass transition of polyethylene chains.  $\alpha$  relaxation is ascribed to the micro-Brownian molecular motion of long segments in the polymer matrix containing the ionic groups of ionic clusters<sup>13-15</sup>.

Focusing on  $\gamma$  transition, a similar shaped peak with a maximum around  $-125.7^{\circ}\text{C}$  was observed in neat EMAA and EMAA-LDH nanocomposites. Nevertheless, a slight shift to higher temperatures was found in the EMAA-O-LDH nanocomposite (with the maximum around  $-125.6^{\circ}\text{C}$ ). This effect could be attributed to the formation of an amorphous phase with more restricted mobility.

With respect to the  $\alpha$  relaxation, the temperature associated to this relaxation ( $T_{\alpha}$ ) passed from  $-24^{\circ}\text{C}$  in pure EMAA to  $-20^{\circ}\text{C}$  in EMAA-LDH and to  $-4.4^{\circ}\text{C}$  in EMAA-O-LDH. As mentioned, this relaxation is related to the movements on the

proper ionic cluster region. Thus, this significant increase of the  $T_{\alpha}$  on the EMAA–O-LDH nanocomposite shows the effectiveness of LDH sheets in increasing the thermal stability of the ionic aggregates, in agreement with observations using the DSC technique.

Similar results were obtained when the dynamic mechanical response was analyzed on the shear mode (Figure 8). As shown, on both loss factor and loss storage curves a  $\gamma$  relaxation (around  $-120$  °C) and  $\alpha$  relaxation (around  $60$ °C) were observed. Moreover, another relaxation could be observed around  $-10$ °C ( $\beta$ ). This relaxation results from motions of chain units located in the interfacial region, i.e., the zone between the crystalline and amorphous part of the polymer<sup>16</sup>.

In accordance with the results obtained using the three-point bending tests, the maximum temperature of  $\alpha$  relaxation transition was shifted to the higher values on EMAA nanocomposites. This effect was clearly observed on both  $\tan \delta$  and loss modulus curves and was more significant in EMAA–O-LDH nanocomposites. These observations reconfirmed the significant effects of the LDH particles on the dynamic mechanical response of the EMAA ionomer because of the strong interactions between LDH sheets and the MAA ionic groups of the ionomer.

## CONCLUSION

Organophilization of the LDH particles was necessary to achieve an exfoliation in the EMAA matrix. LDH sheets, which acted as counterions on the ionic aggregates, induced a significant reduction of the melt flow of the EMAA ionomer. The temperature of the order–disorder transition of the ionic aggregates shifted to higher values on the

nanocomposites, passing from 51.3°C for pure EMAA to 54.7°C and 56.0°C for EMAA-LDH and EMAA-O-LDH respectively. Moreover, the ordering of these ionic aggregates on aging was found to occur more quickly because of the effect of the LDH particles.

The storage moduli measured on tensile and shear modes ( $E'$  and  $G'$ ) of neat EMAA increased by adding the LDH particles. This effect was even more significant when the organophilized ones were dispersed into the EMAA matrix.  $T_g$  values followed a similar tendency. A significant increase was achieved in the nanocomposites, mainly with prepared with O-LDH particles. By contrast, the nanocomposites showed lower loss factor values. This result seems to be related to the fact that the nanocomposites exhibit an amorphous phase with a lower molecular mobility.

Based on these results it can be concluded that the organically-modified LDH particles can effectively increase thermal stability and reinforce the EMAA ionomer matrix.

## References

1. Varley, R.J.; der Zwaag, S. *Acta Mater* 2008, 56, 5737.
2. Leroux, F.; Besse J.P. *Chem Mater* 2001, 13, 3507.
3. Hsueh, H.B.; Chen, C.Y. *Polymer* 2003, 44, 5275.
4. Chen, W.; Feng, L.; Qu, B. *Solid State Com* 2004, 130, 259-263.
5. Costa, F.R.; Abdel-Goad, M.; Wagenknecht, U.; Heinrich, G. *Polymer* 2005, 46, 4447.
6. He, F.A.; Zhang, L.M. *Compos Sci Technol* 2007, 67, 3226.

7. Rives, V. Layered Double Hydroxides: Present and Future; Nova Science Publishers; 2001.
8. Ruthesh, K.S.; Hunter, D.L.; Paul, D.R. *Polymer* 2005, 46, 2646.
9. Tatsuya, S.; Masami, O.; Satoshi, Y.; Hiroshi, H. *Compos Part A: Appl Sci Manufact* 2008, 39, 1924.
10. Ardanuy, M.; Velasco, J.I.; Realinho, V.; Arencón, D.; Martínez, M. *Thermochim Acta* 2008, 479, 45.
11. Miyata, S. *Clays and Clay Miner* 1975, 23, 369.
12. Vanhoorne, P.; Register, R.A. *Macromol* 1996, 29, 598.
13. Tadano, K.; Hirasawa, E.; Yamamoto, J.; Yano, S. *Macromol* 1989, 22, 226.
14. Kutsumizu, S.; Tadano, K.; Matsuda, Y.; Goto, M.; Tachino, H.; Hara, H.; Hirasawa, E.; Tagawa, H.; Muroga, Y.; Yano, S. *Macromol* 2000; 33; 9044.
15. Tachino, K.; Hara, H.; Hirasawa, E.; Kutsumizu, S.; Tadano, K.; Yano, S. *Macromol* 1993, 26, 752.
16. Rodríguez-Pérez, M.A. *Cell Polym* 2002, 21, 117.

**Table 1.** Values of temperature and enthalpy of the order–disorder transition peak after various aging times.

Aging time (min)	EMAA		EMAA-LDH		EMAA-OLDH	
	T (°C)	$\Delta H$ (J/g)	T (°C)	$\Delta H$ (J/g)	T (°C)	$\Delta H$ (J/g)
5	36,7	3,3	36,3	3,9	38,4	2,5
10	38,1	4,8	37,6	5,2	39,4	3,4
40	40,4	7,6	41,0	7,1	42,7	5,9
240	44,8	9,7	45,0	10,4	46,8	10,2
840	47,4	12,5	48,4	13,3	50,1	13,2
172800	58,3	19,5	63,4	21,9	65,6	24,5

**Table 2.** Storage modulus ( $E'$  and  $G'$ ) and loss factor values ( $\tan \delta$ ) from the isothermal DMTA experiments obtained in the three-point bending and shear modes at 1 Hz and  $23 \pm 2^\circ\text{C}$ .

Material	Three-point bending mode		Shear mode	
	$E'$ (MPa)	$\tan \delta$	$G'$ (MPa)	$\tan \delta$
EMAA	293(41)	0.1074 (0.003)	205 (12)	0.0889 (0.005)
EMAA-LDH	307 (9)	0.0835 (0.003)	208 (6)	0.0885 (0.005)
EMAA-OLDH	392 (19)	0.0745 (0.004)	227 (5)	0.0800 (0.005)

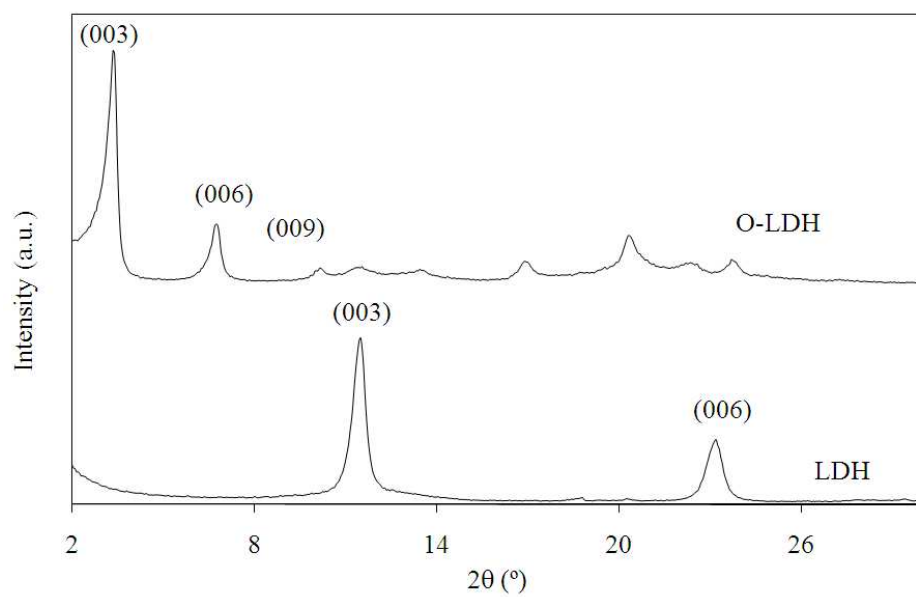


Fig. 1. XRD patterns of LDH and O-LDH particles.  
341x208mm (72 x 72 DPI)

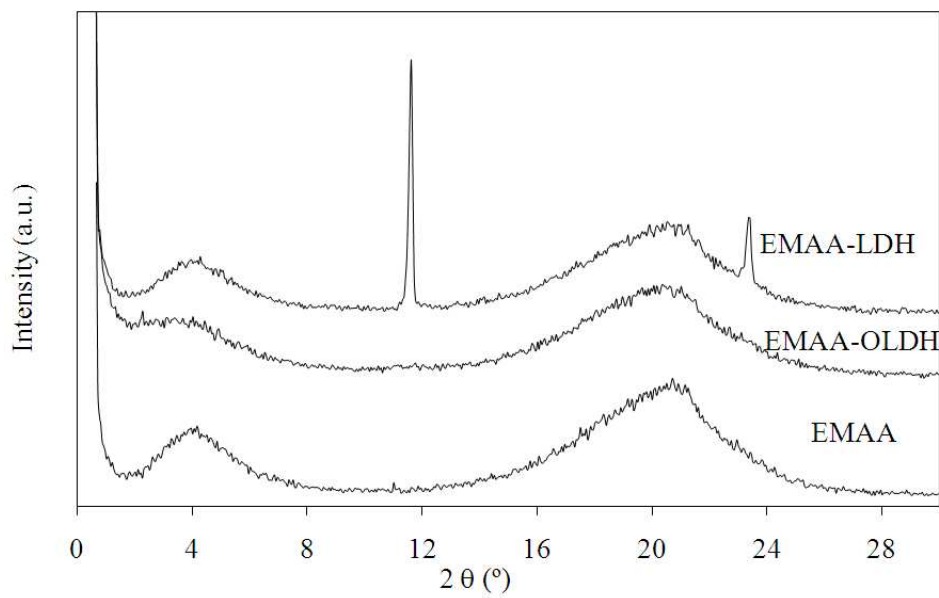


Fig. 2. XRD patterns of EMAA and EMAA nanocomposites.  
330x208mm (72 x 72 DPI)

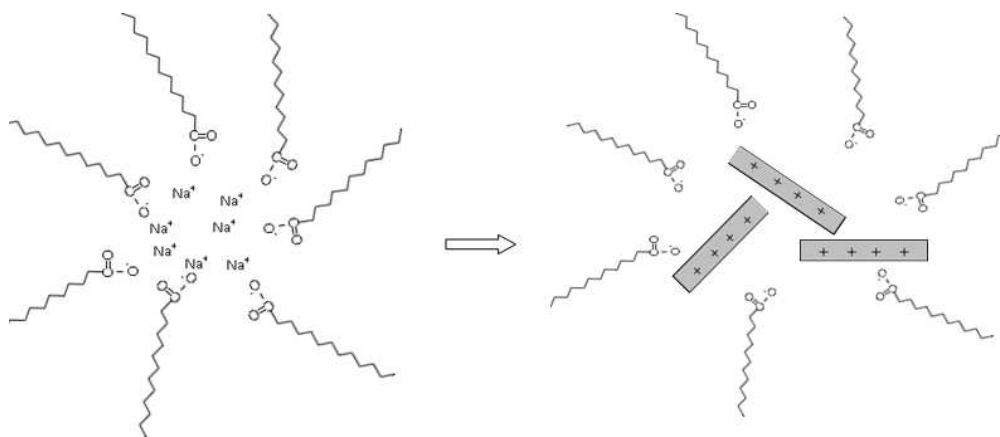


Fig. 3. Schematic illustration of the exchange of sodium ions by the LDH sheets in the ionic clusters.  
210x101mm (96 x 96 DPI)

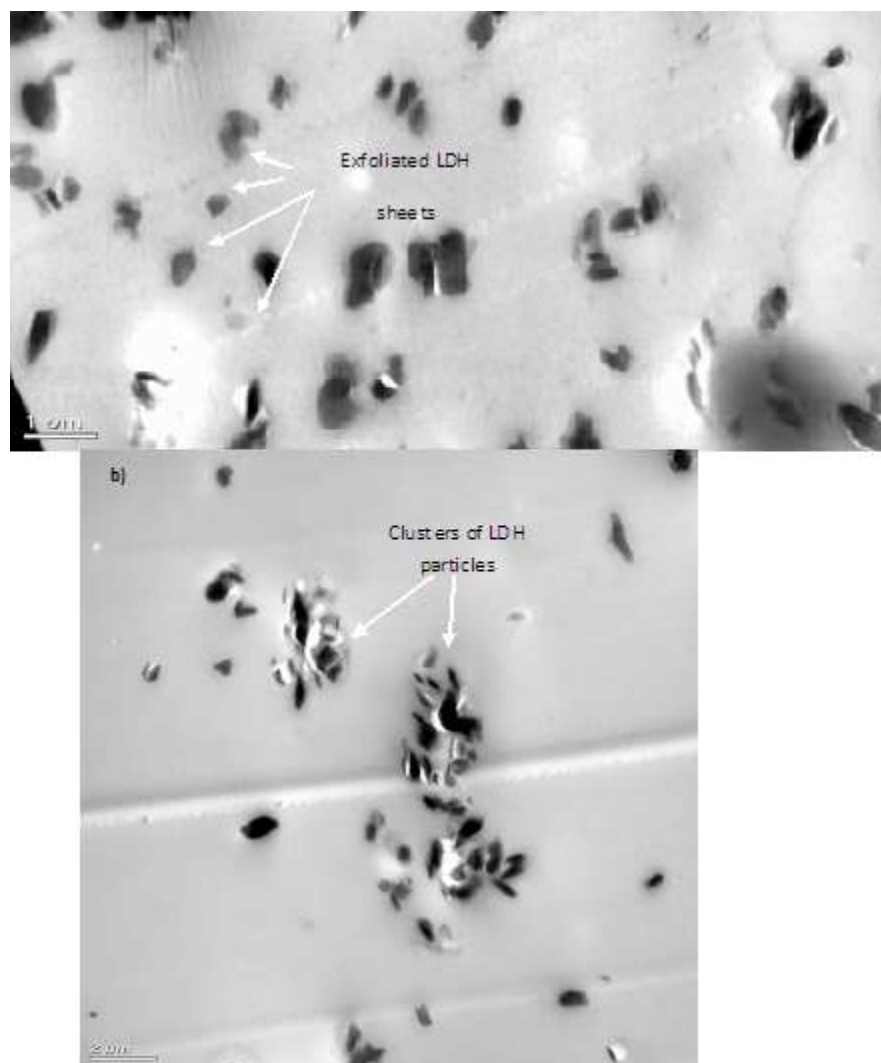


Fig. 4. TEM images of the a) general morphology of EMAA composites and b) detail of the clusters of LDH particles in composites.  
155x186mm (72 x 72 DPI)

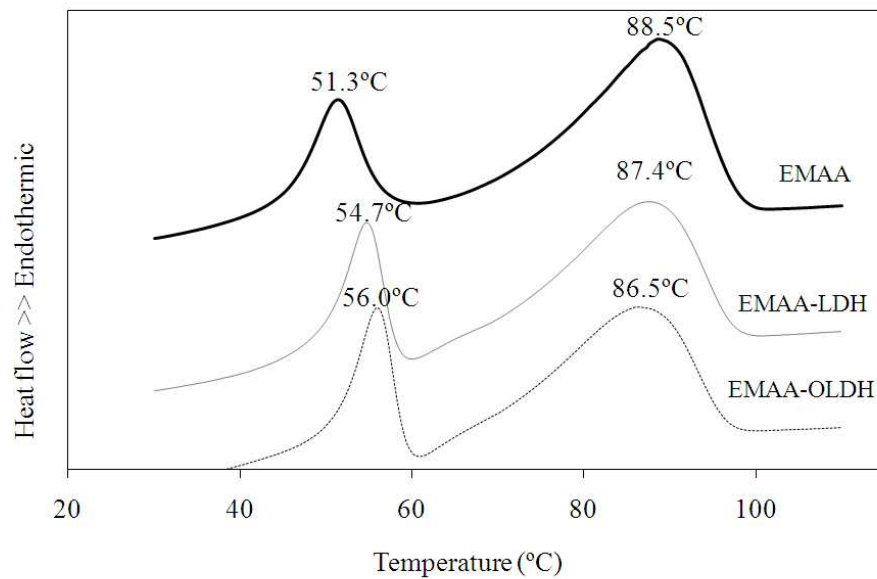


Fig. 5. DSC endotherms of aged EMAA and EMAA nanocomposites, at a heating rate of 10°C/min.  
345x222mm (72 x 72 DPI)

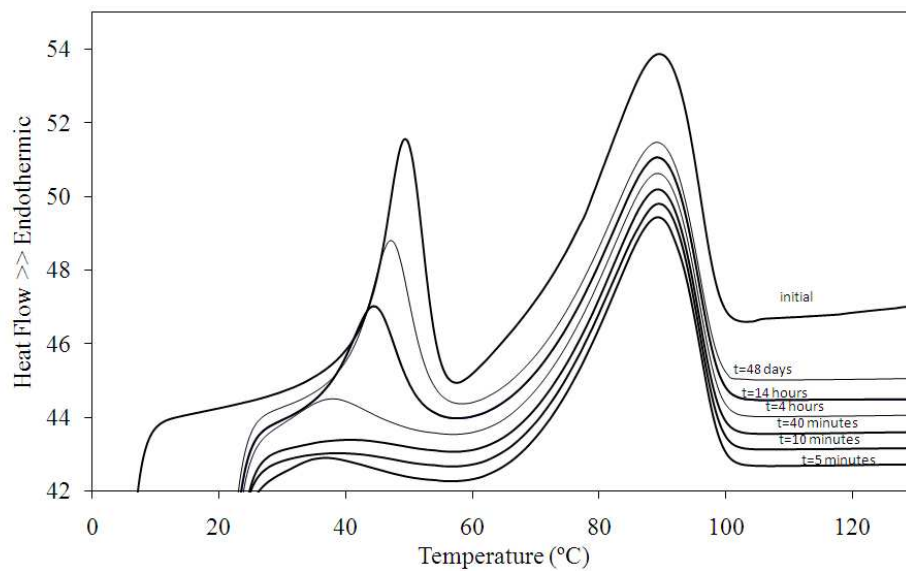


Fig. 6. DSC endotherms of EMAA and EMAA nanocomposites obtained after different annealing periods at 20°C (initial, 5 min, 10 min, 40 min, 4 h, 14 h and 120 d).  
341x208mm (72 x 72 DPI)

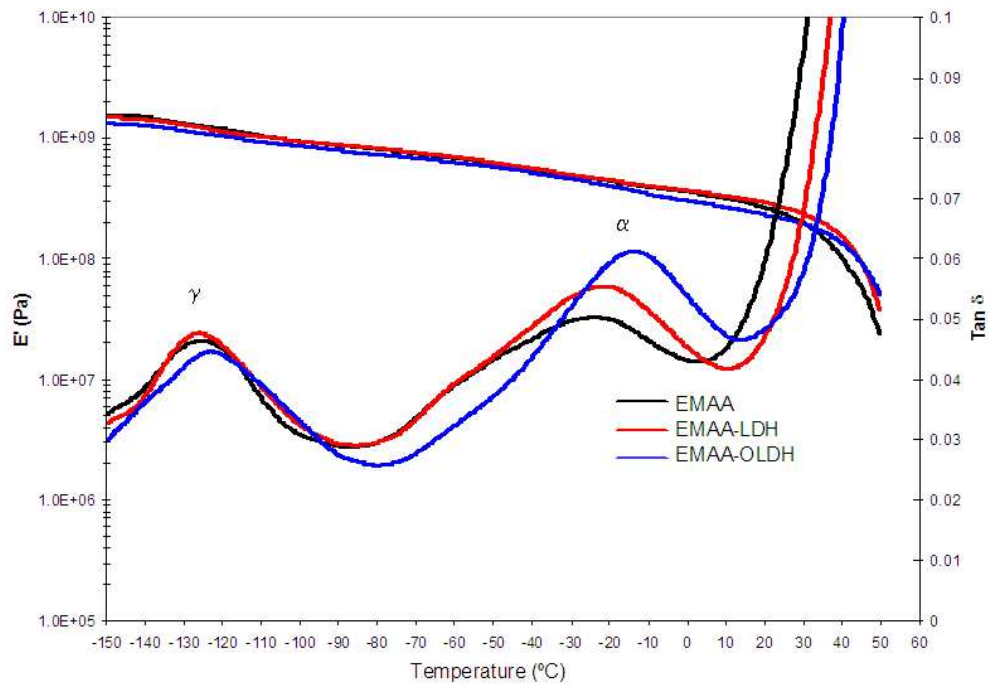


Fig. 7. Variation of the dynamic storage modulus ( $E'$ ) and loss factor value ( $\tan \delta$ ) with temperature of EMAA and EMAA nanocomposites, measured on the three-point bending mode.  
279x236mm (72 x 72 DPI)

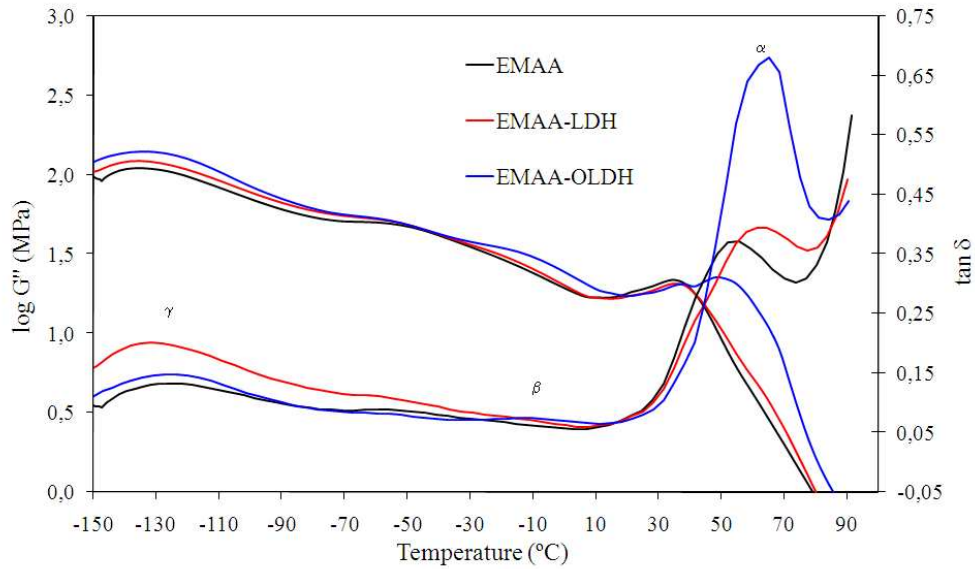


Fig. 8. Variation of the loss modulus ( $G''$ ) and loss factor value ( $\tan \delta$ ) with temperature of EMAA and EMAA nanocomposites, measured on the shear mode.  
341x208mm (72 x 72 DPI)